Second-order photon correlation measurement with picosecond resolution using frequency upconversion

Aymeric Delteil, Chun Tat Ngai, Thomas Fink, Ataç İmamoğlu

Second-order photon correlation measurement with picosecond resolution using frequency upconversion

Aymeric Delteil[1,2], Chun Tat Ngai[1,3], Thomas Fink[1], and Ataç İmamoğlu[1]
1 Institute of Quantum Electronics, ETH Zurich, CH-8093 Zurich, Switzerland.
2 Groupe d'Étude de la Matière Condensée, Université de Versailles Saint-Quentin-en-Yvelines, CNRS UMR 8635, Université Paris-Saclay, 45 Avenue des États-Unis, 78035 Versailles cedex, France
3 Department of Physics, University of Basel, Klingelbergstrasse 82, 4056 Basel, Switzerland
** Corresponding author: aymeric.delteil@uvsq.fr*

The second-order correlation function of light $g^{(2)}(\tau)$ constitutes a pivotal tool to quantify the quantum behavior of an emitter and in turn its potential for quantum information applications. The experimentally accessible time resolution of $g^{(2)}(\tau)$ is usually limited by the jitter of available single photon detectors. Here, we present a versatile technique allowing to measure $g^{(2)}(\tau)$ from a large variety of light signals with a time resolution given by the pulse length of a mode-locked laser. The technique is based on frequency upconversion in a nonlinear waveguide, and we analyze its properties and limitations by modeling the pulse propagation and the frequency conversion process. We measure $g^{(2)}(\tau)$ from various signals including light from a quantum emitter – a confined exciton-polariton structure – revealing its quantum signatures at a scale of a few picoseconds and demonstrating the capability of the technique.

PACS numbers:

The signature of single photon emission is a vanishing second-order correlation function $g^{(2)}(\tau)$ at zero delay ($\tau = 0$). Beyond being one of the most remarkable non-classical properties of light emitted by quantum systems, such behavior also turns out to be an essential resource for optical quantum information technologies. Vanishing $g^{(2)}(0)$ has been consistently observed in emission from a wide variety of physical systems, from single atoms to solid state emitters [1–3], and is typically measured by recording a histogram of the time delays between pairs of photon detection events. In continuous-wave (cw) emission, the timescale at which $g^{(2)}(\tau)$ recovers classical characteristics is in most cases comparable with the lifetime of the emitter excited state. Therefore, the observation of non-classical signatures in $g^{(2)}(\tau)$ is limited to the cases where the resolution of available single-photon detectors (typically several tens to hundreds of picoseconds) is shorter than this characteristic timescale.

In order to overcome this limitation, alternative techniques can be used. Streak cameras provide time resolutions of order picosecond or lower, but their very low repetition rate ($\lesssim 1$ kHz) precludes their use for measuring two-photon correlations of weak signals [4, 5]. On another note, frequency conversion using a short laser pulse can also provide high time resolution [6]. This technique has been used to characterize the fluorescence decay of a wide range of physical systems under pulsed excitation, with a resolution below a picosecond [7–10]. In these experiments, the emitted light is mixed in a nonlinear crystal with a short laser pulse (termed pump pulse) that is synchronized with the excitation laser. Since frequency conversion occurs only during the pump pulse, the latter serves as a fast gate that provides accurate information about the emission time. The converted photons are then detected by standard detectors, and the signal envelope is reconstructed by recording the detection rate while varying the time delay between the signal and pump pulses. Recent progress in the conversion efficiency of nonlinear crystals based on QPM has allowed time-resolved detection of single-photons generated by spontaneous parametric downconversion [11] and realization of fast gating of quantum dot single-photon emission [12–14] based on the same principle.

Here, we extend the principle of these experiments to the measurement of the second-order correlation function of arbitrary light signals. When the signal is synchronized with the pump laser, our technique gives access to the two-time second order correlation $g^{(2)}(t_1, t_2)$. In the opposite case of continuous wave light sources, our method realizes a Hanbury Brown and Twiss measurement, allowing us to extract $g^{(2)}(\tau)$ with picosecond time resolution. The nonlinear medium we use is a periodically poled lithium niobiate (PPLN) crystal waveguide with intrinsically high conversion efficiency, allowing for measurement of very weak signals down to the single photon level. Thanks to the waveguide configuration, the QPM condition can be fulfilled by simply tuning the wavelength of the pump laser. Consequently, a wide range of signal wavelengths can be measured using the same set-up. Our technique is expected to play a crucial role for characterizing the purity and indistinguishability of ultrafast single photon sources with a radiative decay rate exceeding the bandwidth of single photon detectors, based for instance on confined exciton-polaritons [15, 16] or single emitters in microcavities and plasmonic structures [17, 18].

The setup is depicted in figure 1a. It is based on a Ti:sapphire (pump) laser of pulse length 2.5 ps and repe-

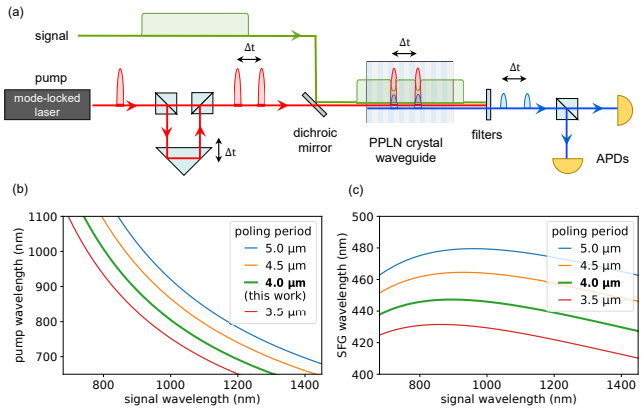

FIG. 1: (a) Experimental set-up. Two ps-pulses (red beam) with variable delay are mixed with an input signal (green beam) in a PPLN crystal waveguide. The upconverted pulses (blue beam) are detected in a Hanbury Brown and Twiss setup. (b) Pump wavelength as a function of the signal wavelength calculated from the phase-matching relations in PPLN with various poling period. (c) Corresponding final wavelength as a function of the signal wavelength.

tition rate 76 MHz from which we generate pairs of pulses separated by a variable delay. A dichroic mirror combines the pump pulses and the input signal into a single spatial mode, which is focused on the input facet of a commercial PPLN waveguide (from HC Photonics) of poling period 3.96 μm, length 12.5 mm and mode size 4 μm×6 μm. The polarization of both the pump and the signal are made parallel to the extraordinary axis of the PPLN crystal. Provided that the pump wavelength is tuned to be in quasi-phase matching (QPM) condition with the signal wavelength, sum frequency generation (SFG) occurs in the PPLN waveguide (figure 1b). The tunability range of our pump laser allows QPM for signal wavelength from 750 nm to 1150 nm and could be extended further by choosing a different poling period of the PPLN crystal (figure 1b). The upconverted signal wavelength depends only weakly on the signal wavelength and is about 445 nm (figure 1c). After filtering out the signal, pump pulse, and its second harmonic from the output of the waveguide, the upconverted pulses are collected in the input port of a fiber beamsplitter. The two output ports are coupled to standard avalanche photodiodes (APDs) of time resolution $\sim$ 300 ps. The coincidence rate $C(\Delta t)$ is recorded as a function of the time delay Δt between the pulses. $C(\Delta t)$ is then normalized by the average coincidence rate between pairs of photons originating from different (uncorrelated) pump pulse periods, which yields $c(\Delta t) = C(\Delta t)/\langle C(\Delta t + nT)\rangle_{n\neq 0}$, where T is the repetition rate of the pump laser. Note that $C(\Delta t)$ contains equal contributions from photon pairs converted by the same pump pulse and by the two different pump pulses. Therefore, the resulting normalized coincidence rate reads $c(\Delta t) = \frac{1}{2}\left(g^{(2)}(\Delta t) + g^{(2)}(0)\right)$. The second order correlation function can then be retrieved straightforwardly as: $g^{(2)}(\Delta t) = 2c(\Delta t) - c(0)$.

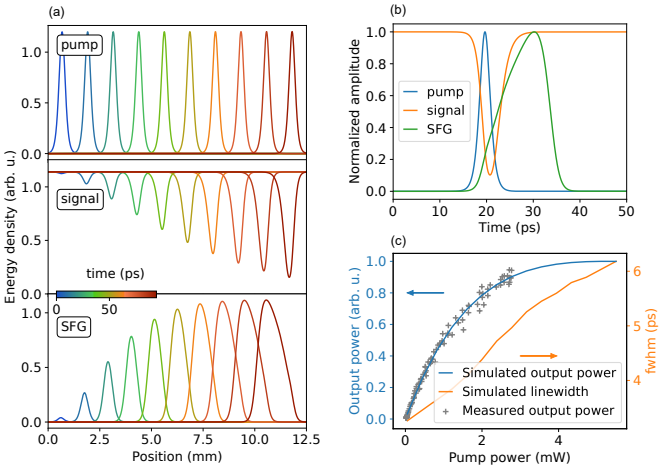

FIG. 2: (a) Spatial envelope of the pump (upper panel), the signal (middle panel), and the SFG (lower panel) at various propagation times, indicated by the color scale. The span of the x axis is equal to the waveguide length. (b) Normalized temporal envelope of the three output pulses. The FWHM of the dip in the signal envelope provides the time resolution of our setup. (c) Continuous curves: calculated output power (blue curve) and time resolution (orange curve) as a function of the pump power. Crosses: measured output power as a function of the pump power.

The limitations to the time resolution of the setup can be identified by simulating the pulse propagation and frequency conversion in the waveguide. We implemented a 1D propagation model that is detailed in the Appendix A. We model the pump pulse by a sech-squared pulse of width 2.5 ps as determined from pulse autocorrelation measurements, while the signal is initially taken as constant. Figure 2a shows the results of the simulations. The pump peak power is taken much higher than the signal power. Under this assumption, the pump pulse remains essentially undepleted as it propagates along the crystal (upper panel). The signal envelope (middle panel) exhibits a dip originating from upconverted photons during the sampling process. The width of the dip therefore provides the time range that has been probed during the upconversion process, *i.e.* the time resolution of the measurement. In the ideal case of a signal and pump having the same group velocity, the pump pulse and the signal dip would keep a perfect overlap during propagation, ensuring a time resolution limited by the pump pulse width. In our case however, the group velocity difference between the pump and signal is finite, leading to a sizable broadening of the dip. Finally, the SFG (lower panel) propagates at a much smaller group velocity compared to the signal and pump, leading to a broadened and delayed SFG pulse, however without impacting the time

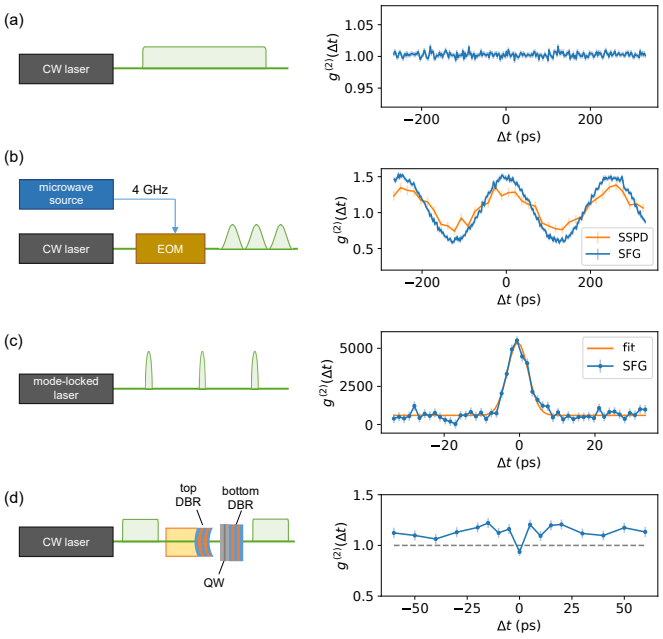

FIG. 3: Experimental $g^{(2)}(\Delta t)$ for various input signals. (a) CW laser, (b) CW laser modulated at 4 GHz by an EOM (blue curve). The orange curve is the $g^{(2)}(\Delta t)$ of the same signal measured with a SSPD of time resolution ~ 40 ps. (c) ps-laser with a repetition rate incommensurable with the pump. The orange curve is a Gaussian fit to the data. (d) Light transmitted through a confined polariton structure. QW: quantum well; DBR: distributed Bragg mirror.

resolution. Figure 2b shows the temporal envelope of the three waves at the output of the 12.5 mm waveguide. The width of the dip in the signal envelope provides the time resolution of the setup, which we find to be 4.0 ps, primarily limited by the pump pulse length (2.5 ps), but also by the group velocity difference between pump and signal, and the upconversion saturation that leads to additional broadening. Figure 2c shows the pump power dependence of the integrated upconverted signal (blue curve) and time resolution of the setup, given by the FWHM of the signal dip (orange curve). The output power exhibits a saturation behavior accompanied with a broadening of the resolution. The experimental conversion efficiency presents the same saturation behavior, allowing us to fit the saturation power (or equivalently the conversion efficiency) in the model. The final choice of the pump power results from a trade-off between conversion efficiency and time resolution. In the following, we set the pump power to be 1.5 mW, corresponding to the parameters used in the calculations of figure 2a and b.

In order to characterize the performance of our setup, we first perform autocorrelation of classical signals – lasers with time-varying envelope – to infer the properties and illustrate the capabilities of our system. To this end, the signal source is not synchronized with the measurement pump laser, such that we directly access $g^{(2)}(\tau) = \left\langle g^{(2)}(t, t+\tau)\right\rangle_t$. Figure 3 displays the measurement results with various input signals. We start with cw laser light at a wavelength of 812 nm. The pump laser is tuned to 990 nm to obtain QPM. The result is shown fig. 3a: As expected, the measured $g^{(2)}$ is flat over the whole range, with a mean value of 1.00 ± 0.01, ensuring absence of specious correlations from the setup. The blue curve in fig. 3b shows the $g^{(2)}$ of a cw laser that is modulated at 4 GHz using an electro-optical modulator (EOM). The modulation frequency is incommensurable with the pump repetition rate. The $g^{(2)}$ exhibits oscillations of visibility 38 %, corresponding to half of the modulation depth of the EOM. We compare with the result obtained with a superconducting single-photon detector (SSPD) of resolution ∼40 ps per channel (including electronics) using a standard start-stop technique (orange curve in fig. 3b). In the latter case we observe similar oscillations, with reduced visibility of 26 %, limited by the resolution of the SSPD. In order to estimate the resolution of our system, we then use the signal from a ps-laser of pulse length 2.5 ps and wavelength 812 nm as an input. The repetition rates of the signal and pump laser are incommensurable [**?**]. We obtain a peak centered at zero delay with a linewidth of 6.5 ± 0.1 ps as extracted from a Gaussian fit to the data (see fig. 3c). We deduce the resolution of the upconversion setup to be 4 ± 0.5 ps, in agreement with our simulations. In the last step, we feed our setup with a source of weakly subpoissonian light. The emitter consists of a resonantly driven fiber cavity in strong coupling with the excitonic transition of a single quantum well. The structure and the optical setup are extensively described in ref [16] and sketched in fig. 3d. This source emits weakly antibunched light on top of a bunched background when weakly excited with a negative laser detuning of about half the mode linewidth [15, 16]. The result we found is in agreement with the data previously acquired in a pulsed regime [16], unveiling the different timescales associated with the antibunched (visible for $\Delta t < 20$ ps) and bunched (persisting for $\Delta t > 50$ ps) components [**?**]. Although the minimum of antibunching $g^{(2)}(0) = 0.94 \pm 0.04$ is close to the classical limit, the most striking non-classical property revealed by our data is the violation of the classical inequality $g^{(2)}(0) \geq g^{(2)}(\tau)$ [19]. In our case the value of $g^{(2)}(0)$ lies below the maximum of $g^{(2)}(\Delta t)$ by more than 4 standard deviations, confirming the non-classical nature of the source from a time-resolved approach.

The resolution of our setup is limited both by the length of the pump pulse and the propagation and conversion saturation in the PPLN crystal. It is however straightforward to further improve it by at least one order of magnitude by using femtosecond pulses together with a shorter crystal (see Appendix B). The overall efficiency of $5.3 \cdot 10^{-6}$ is mainly limited by the ratio between the pulse width and the repetition period (see Appendix C for de-

tailed contributions to the detection efficiency). Given the noise level during our detection window, this corresponds to a noise equivalent power of about 0.3 pW. Although this level is frequently exceeded by solid-state quantum emitters in cavities, additional effort is needed to extend the range of systems to which our technique can be applicable. The quantum efficiency could be increased with a higher repetition rate of the pump laser, as long as the corresponding pulse period is longer than the APD time resolution. Amongst the existing techniques allowing to measure $g^{(2)}(\tau)$ with picosecond resolution or lower, the techniques based on homodyne detection possess similar intrinsic limitations since the signal is probed only during a pair of laser pulses that provide the desired time resolution [20]. Alternatively, two-photon absorption can also provide very high time resolution but has been shown to yield measurable outcome only for input signal of about a microwatt or more [21]. Although synchronization between pump and signal is not needed to measure $g^{(2)}(\tau)$, it is also possible to excite the signal emitter in a synchronous way, allowing to measure two-time correlation function $g^{(2)}(t_1, t_2)$ in a dynamical or transient regime [22, 23].

To conclude, the technique we developed for photon correlation measurements based on ultrafast light sampling is likely to play an increasingly important role in the measurement of quantum optical properties of ultrafast single photon sources [24], as well as in the investigation of single- or few-photon phenomena in condensed matter occurring at short timescales [25–27]

Funding. Swiss National Science Foundation (SNSF) through a DACH project 200021E-158569-1; SNSF National Centre of Competence in Research - Quantum Science and Technology (NCCR QSIT); ERC Advanced investigator grant (POLTDES).

Acknowledgment. The Authors gratefully acknowledge many enlightening discussions with K. Srinivasan. They also thank A. Schade, C. Schneider and S. Höfling for the growth of the sample used to obtain the data depicted in Fig. 3d.

Appendix

Simulation of the pulse propagation and upconversion

We start from the wave equation in a lossless nonlinear medium [28]:

$$\nabla^2\mathbf{E} - \varepsilon\frac{\partial^2\mathbf{E}}{\partial t^2} = \frac{\partial^2\mathbf{P}_{\mathrm{NL}}}{\partial t^2}$$

with, in our case:
$\mathbf{E} = E_z\mathbf{z}$, $E_z = E_{\mathrm{P}} + E_{\mathrm{S}} + E_{\mathrm{SFG}}$. Here, P denotes the pump, S the signal and SFG the sum frequency generation.
$E_i = 1/2\,(A_i(z,t)\exp(i(\omega t - k_i z)) + c.c.)$ with i =P, S, SFG;
and $\mathbf{P}_{\mathrm{NL}} = \varepsilon\chi^{(2)}E^2$
We derive time-dependent equations for the envelope functions $A_i(z,t)$ under the assumptions of slow-varying envelope and negligible losses. We obtain a system of coupled first-order wave equations for the envelope functions, that we numerically solve using the following initial conditions at $t = 0$ for the three waves:

- Pump: sech-square pulse of width 2.5 ps, spatially centered at $z = 0$ (input facet of the waveguide) $A_{\mathrm{P}} = A_{\mathrm{P},0}\ \mathrm{sech}\left(\dfrac{z}{v_{\mathrm{g,P}}\tau_{\mathrm{P}}}\right)$ with τ_{P} =FWHM/1.76
- Signal: constant signal $A_{\mathrm{S}}(z) = A_{\mathrm{S},0}$
- SFG: $A_{\mathrm{SFG}}(z) = 0$

The optical indices and group velocities are calculated from the Sellmeyer equations for lithium niobiate [29]. The periodically poled medium is modeled by using $d = d_{\mathrm{eff}}(z)$ of constant magnitude and alternating sign. The magnitude $|d|$ is chosen to reproduce the experimental saturation of the upconverted signal (shown fig 2c of the main text).

Femtosecond upconversion

We have performed simulations of a 1 mm long PPLN crystal with a pump pulse length of 200 fs and average power 0.5 mW, chosen such that the conversion efficiency is similar to the picosecond case. We deduce from the FWHM of the dip in the signal envelope that the time resolution of the upconversion process is 300 fs, mainly limited by the group velocity mismatch between the pump and the signal. The effects of pulse dispersion are negligible. Even shorter resolution could in principle be reached using shorter pump pulses, a smaller crystal length and possibly a different choice of poling period that would minimize the group velocity difference.

Detection efficiency of the setup

The efficiency of our setup can be estimated from the count rate of the upconverted photons obtained from a given input signal power. A cw input of 22 nW at 845 nm leads to $5\cdot10^5$ photon counts/s in the APDs, which yields $5.3\cdot10^{-6}$ overall quantum efficiency. The main contribution is the low duty cycle of the pump laser of 2.5 ps/13 ns $= 1.9\cdot10^{-4}$. Other contributions include coupling to the waveguide (0.3), coupling of the upconverted photons to the output fiber (0.5) and conversion efficiency of the APDs at 440 nm (0.25) from which we deduce an average conversion efficiency of about 0.75 in the waveguide

during the 2.5 ps pump pulse. Increasing the conversion efficiency further leads to a degradation of the time resolution, as shown on Fig. 2c of the main text.

[1] P. Grangier, G. Roger, and A. Aspect, Europhysics Letters **1**, 173 (1986).

[2] B.Lounis and W. Moerner, Nature **407**, 491 (2000).

[3] I. Aharonovich, D. Englund, and M. Toth, Nature Photonics **10**, 631 (2016).

[4] M. Ueda, M. Kuwata, N. Nagasawa, T. Urakami, Y. Takiguchi, and Y. Tsuchiya, Optics Communications **65**, 315 (1988).

[5] M. Aßmann, F. Veit, J.-S. Tempel, T. Berstermann, H. Stolz, M. van der Poel, J. M. Hvam, and M. Bayer, Optics Express **18**, 20229 (2010).

[6] H. Mahr and M. D. Hirsch, Optics Communications **13**, 96 (1975).

[7] D. Block, J. Shah, and A. Gossard, Solid State Communications **59**, 527 (1986).

[8] J. Shah, IEEE Journal of Quantum Electronics **24**, 276 (1988).

[9] A. Mokhtari, J. Chesnoy, and A. Laubereau, Chemical Physics Letters **155**, 593 (1989).

[10] P. Changenet-Barret, T. Gustavsson, R. Improta, and D. Markovitsi, Journal of Physical Chemistry A **119**, 6131 (2015).

[11] O. Kuzucu, F. N. C. Wong, S. Kurimura, and S. Tovstonog, Optics Letters **33**, 2257 (2008).

[12] M. T. Rakher, L. Ma, M. Davanc, O. Slattery, X. Tang, and K. Srinivasan, Physical Review Letters **107**, 083602 (2011).

[13] K. D. Greve, L. Yu, P. L. McMahon, J. S. Pelc, C. M. Natarajan, N. Y. Kim, E. Abe, S. Maier, C. Schneider, M. Kamp, et al., Nature **491**, 421 (2012).

[14] L. Yu, C. M. Natarajan, T. Horikiri, C. Langrock, J. S. Pelc, M. G. Tanner, E. Abe, S. Maier, C. Schneider, S. Höfling, et al., Nature Communications **6**, 8955 (2015).

[15] G. Munoz-Matutano, A. Wood, M. Johnsson, X. Vidal, B. Q. Baragiola, A. Reinhard, A. Lemaître, J. Bloch, A. Amo, G. Nogues, et al., Nature Materials **18**, 213 (2019).

[16] A. Delteil, T. Fink, A. Schade, S. Höfling, C. Schneider, and A. İmamoğlu, Nature Materials **18**, 219 (2019).

[17] M. Bayer, T. L. Reinecke, F. Weidner, A. Larionov, A. McDonald, and A. Forchel, Physical Review Letters **86**, 3168 (2001), URL `https://link.aps.org/doi/10.1103/PhysRevLett.86.3168`.

[18] T. B. Hoang, G. M. Akselrod, and M. H. Mikkelsen, Nano Letters **16**, 270 (2016).

[19] R. Loudon, *The Quantum Theory of Light* (Clarendon Press, Oxford, 1973).

[20] D. F. McAlister and M. G. Raymer, Physical Review A **55**, R1609 (1997).

[21] F. Boitier, A. Godard, E. Rosencher, and C. Fabre, Nature Physics **5**, 267–270 (2009).

[22] B. D. Mangum, Y. Ghosh, J. A. Hollingsworth, and H. Htoon, Optics Express **21**, 7419 (2013).

[23] F. Eloi, H. Frederich, A. Leray, S. Buil, X. Quélin, B. Ji, E. Giovanelli, N. Lequeux, B. Dubertret, and J.-P. Hermier, Optics Express **23**, 29921 (2015).

[24] T. B. Hoang, G. M. Akselrod, C. Argyropoulos, J. Huang, D. R. Smith, and M. H. Mikkelsen, Nature Communications **16**, 7788 (2015).

[25] H. Snijders, J. Frey, J. Norman, H. Flayac, V. Savona, A. Gossard, J. Bowers, M. van Exter, D. Bouwmeester, and W. Löffler, Physical Review Letters **121**, 043601 (2016).

[26] P. Tighineanu, R. S. Daveau, T. B. Lehmann, H. E. Beere, D. A. Ritchie, P. Lodahl, and S. ren Stobbe1, Physical Review Letters **116**, 163604 (2016).

[27] Y. L. Delley, M. Kroner, S. Faelt, W. Wegscheider, and A. İmamoğlu, Physical Review B **96**, 241410 (2017).

[28] R. W. Boyd, *Nonlinear Optics (3rd edition)* (Academic Press, 2008).

[29] O. Gayer, Z. Sacks, E. Galun, and A. Arie, Applied Physics B **91**, 343 (2008).